Ab initio calculations of structural and electronic properties of 6*H*-SiC(0001) surfaces

Magdalena Sabisch, Peter Krüger, and Johannes Pollmann
Institut für Theoretische Physik II–Festkörperphysik, Universität Münster, D-48149 Münster, Germany
(Received 13 December 1996)

We report *ab initio* calculations of structural and electronic properties of hexagonal 6*H*-SiC(0001) surfaces. The calculations have been carried out self-consistently within a local density approximation employing supercell geometries, smooth norm-conserving pseudopotentials in separable form and Gaussian orbital basis sets. In a systematic study, we have investigated the relaxation, as well as $(\sqrt{3}\times\sqrt{3})R30°$ reconstructions of both Si- and C-terminated substrate surfaces. We have optimized eight structural models for the reconstructed surfaces with Si or C adatoms and Si or C trimers adsorbed in threefold-symmetric T_4 or H_3 positions. In the case of the Si-terminated substrate surface, our results favor Si adatoms in T_4 sites as the optimal configuration which is compatible with structure data from experiment. For the C-terminated substrate surface, our results indicate that none of the investigated $\sqrt{3}\times\sqrt{3}$ adatom or trimer configurations is the optimal surface structure. We present the electronic structure of the relaxed and of some representative reconstructed surfaces and discuss our results in comparison with other theoretical results and with experimental data from the literature. [S0163-1829(97)00816-3]

I. INTRODUCTION

Polar (0001) surfaces of the technologically very important semiconductor compound 6*H*-SiC are attracting considerable interest in recent years.[1–3] The clean, ideal 6*H*-SiC(0001) surfaces are either Si or C terminated. Since many reconstruction models for the (0001) surfaces involve adatoms, we refer to them in the following as Si- or C-terminated substrate surfaces. They are characterized by Si (C) top-layer atoms with one dangling bond and three back bonds connecting them with their three nearest-neighbor C (Si) atoms on the second substrate layer. While experiment can distinguish between different substrate-surface terminations, an absolute determination of the Si face or the C face seems difficult.[3] The stacking sequence of Si-C bilayers in the hexagonal [0001] direction of 6*H*-SiC and in the cubic [111] direction of β-SiC differs only beginning with the ninth layer. Because of this fact, experimental low-energy electron diffraction (LEED), Auger electron spectroscopy (AES), and electron energy loss spectroscopy (EELS) results are almost identical for respective reconstructions of the β-SiC(111) and the 6*H*-SiC(0001) surface when using electrons with low energy.[4] Based on the indistinguishable LEED results one can conclude that the surfaces are characterized by the same reconstruction geometry. The Si- and C-terminated β-SiC(111) and 6*H*-SiC(0001) surfaces have been and still are investigated very intensively by LEED,[4–9] AES,[4–8,10] scanning tunneling microcospy (STM),[7,9,11–14] atomic force microscopy (AFM),[15] EELS,[4,7,10] x-ray photoelectron spectroscopy (XPS),[6,10,16] angle-resolved photoelectron spectroscopy (ARPES),[17] and *k*-resolved inverse photoelectron spectroscopy (KRIPES).[18] Among the structures reported are (1×1), $\sqrt{3}\times\sqrt{3}$, (3×3), $6\sqrt{3}\times6\sqrt{3}$, and (9×9) configurations depending sensitively on temperature and on sample preparation. The $\sqrt{3}\times\sqrt{3}$ and $6\sqrt{3}\times6\sqrt{3}$ reconstructions involve 30° rotations of the unit cell and are $R30°$ reconstructions therefore. These reconstructions are thought to originate from adsorbed Si or C adatoms or Si or C trimers and are thus interpreted as adsorption-induced reconstructions.

Different preparation methods appear to yield different reconstructions.[3] LEED patterns show an unreconstructed (1×1) structure up to 800° and various reconstructions after annealing at 900–1100 °C.[6] Chemical treatment in *HF* (Ref. 6) or buffered *HF* (Refs. 7 and 8) removes the oxide and passivates the surface. Annealing up to 900–1000 °C in UHV results in a $\sqrt{3}\times\sqrt{3}$ reconstruction for the Si-terminated surface[6,7,9] and in a 3×3 reconstruction[6] for the C-terminated surface. Further annealing above 1000 °C causes a Si depletion and graphitization of the surface leading to a $6\sqrt{3}\times6\sqrt{3}$ reconstruction.[5,9,12,13] Bermudez has prepared clean (0001) surfaces by annealing in a flux of Si vapor and observes a (3×3) structure for the Si-terminated surface which converts to $(\sqrt{3}\times\sqrt{3})R30°$ upon further annealing in vacuum.[3] The author has observed that the (3×3) surface consists of an ordered layer of Si chemisorbed on the Si substrate surface layer while the $(\sqrt{3}\times\sqrt{3})R30°$ reconstruction involves an ordered arrangement of Si vacancies. For the C-terminated surface, Bermudez has observed a (1×1) structure which transforms into a poor quality (3×3) structure upon further annealing. Owman and Mårtensson[9] have investigated Si-terminated 6*H*-SiC(0001)-$(\sqrt{3}\times\sqrt{3})R30°$ surfaces by STM. The authors observed images consistent with a structural model composed of 1/3 layer of Si or C adatoms in threefold-symmetric sites above the outermost Si-C bilayer, similar to the reconstructions observed for 1/3 monolayer of, e.g., Al, Ga, In, or Pb on the Si(111) surface.[19–22] Similar structural models had been suggested by Kaplan,[4] before. From STM data alone, it is neither possible to identify which one of the elements (Si or C) constitutes the adatoms nor to determine in which of the two symmetry-allowed sites (T_4 or H_3) the adatoms are located. A mixture of adsorbed Si and C adatoms was excluded in Ref. 9. But more complex structures such as, e.g., trimers could not be excluded. Thus the

authors did not arrive at a definite structural model for the $\sqrt{3}\times\sqrt{3}$ reconstructed surface. Li and Tsong[11] have studied Si- and C-terminated surfaces after annealing at 850–950 °C under a Si flux using STM. On both surfaces the authors observed a (3×3) reconstruction after annealing at 850 °C, which changed into a $\sqrt{3}\times\sqrt{3}$ reconstruction *in both cases* after further annealing at 950 °C. In general, the experimental structure data seem not to be entirely conclusive, yet.

To date, only very few theoretical investigations of polar hexagonal 6*H*-SiC(0001) surfaces have been reported. Badziag[23,24] has carried out semiempirical structure studies of Si- and C-terminated $\sqrt{3}\times\sqrt{3}R30°$ configurations. The author employed semiempirical quantum-chemical cluster calculations of the modified neglect of differential overlap (MNDO) type and arrived at C trimers saturated by hydrogen atoms as the optimal configuration for the Si-terminated surface.[24] For the C-terminated 6*H*-SiC(0001)-$(\sqrt{3}\times\sqrt{3})$ surface Badziag favored a model containing Si adatoms and C atoms substituting for Si in the second layer of the unreconstructed substrate surface.[23] *Ab initio* calculations within local density approximation (LDA) of density functional theory have been reported by Northrup and Neugebauer.[25] These authors have studied Si-terminated β-SiC(111)-$(\sqrt{3}\times\sqrt{3})R30°$ surfaces. As mentioned before, these are largely equivalent to the respective hexagonal surface since the stacking sequence of Si-C bilayers along the [111] direction in β-SiC and along the [0001] direction in 6*H*-SiC, respectively, is equivalent down to the eighth layer. For the Si-terminated substrate surface the authors favored adsorption of Si adatoms in T_4 sites as optimal structure. We have previously presented brief accounts of results of our LDA calculations for the structure and the electronic structure of Si- and C-terminated 6*H*-SiC(0001)-$(\sqrt{3}\times\sqrt{3})R30°$ surfaces.[26,27]

To contribute to the vivid current discussion of the reconstructions of 6*H*-SiC(0001) surfaces, we have systematically studied the relaxed (1×1), as well as a number of reconstructed $\sqrt{3}\times\sqrt{3}$ configurations of both Si- and C-terminated (0001) surfaces of 6*H*-SiC. In this paper we present and discuss a full account of the results of our *ab initio* pseudopotential LDA calculations. We have optimized eight structural models for the reconstructed surfaces with Si or C adatoms and Si or C trimers adsorbed in threefold-symmetric T_4 or H_3 positions. The calculations have been carried out within the supercell approach using smooth pseudopotentials and localized Gaussian orbitals. For the Si- and C-terminated substrate surfaces we present optimal reconstruction configurations of the investigated structure models and for some representative configurations we present and discuss the respective surface electronic structure.

The paper is organized as follows. In Sec. II we briefly summarize the framework of our calculations. Section III is devoted to the presentation of surface structural and electronic properties for both the Si- and the C-terminated relaxed (1×1) substrate surface. In Sec. IV we present and discuss our results for five different configurations with Si or C adatoms and Si or C trimers adsorbed in threefold-symmetric T_4 or H_3 positions at the Si-terminated $\sqrt{3}\times\sqrt{3}$ substrate surface. In addition, we discuss three adatom structures at the C-terminated $\sqrt{3}\times\sqrt{3}$ substrate surface. Our results are compared with those of other calculations and with available experimental data. A summary concludes the paper in Sec. V.

II. CALCULATIONAL FRAMEWORK

Our calculations are carried out in the framework of density-functional theory within the local density approximation.[28] For the exchange and correlation potential we employ the functional of Ceperley and Alder[29] as parametrized by Perdew and Zunger.[30] Nonlocal, norm-conserving pseudopotentials in separable form, as suggested by Kleinman and Bylander,[31] are used. They were generated following the prescription given by Hamann, Schlüter, and Chiang[32] and have been reported elsewhere.[33] Employing our very smooth pseudopotentials in particular for the second row element carbon, the numerical effort is strongly reduced. The wave functions are expanded in terms of linear combinations of Gaussian orbitals with s, p, d, and s^* symmetry. We find that 30 Gaussians per surface-layer atom and 20 Gaussians per atom for all other atoms in the supercell yield sufficient accuracy.[34,35] Using these pseudopotentials and Gaussian orbital basis sets we have successfully investigated the relaxed β-SiC(110)-(1×1) surface[34] and a number of reconstruction models for β-SiC(001) surfaces,[35] previously. The total energy is calculated self-consistently using the momentum-space formalism of Ihm, Zunger, and Cohen.[36] All computations are performed using sets of six $\mathbf{k}_\parallel$ points for the (1×1) unit cell and three $\mathbf{k}_\parallel$ points for the $(\sqrt{3}\times\sqrt{3})R30°$ unit cell in the irreducible part of the surface Brillouin zone (SBZ). Using the supercell method we employ eight layers of SiC, one layer of adatoms, and seven vacuum layers in the supercell. In addition, the broken sp^3 bonds at the bottom layer atoms in each supercell are saturated with one hydrogen atom, each. The lower four atomic layers of SiC are fixed in the bulk configuration employing the theoretical lattice constants $a=3.07$ Å and $c=15.05$ Å. We optimize the structure by calculating the forces. We move the atoms of the upper four substrate layers and the adlayer atoms in the supercell until all forces vanish within 10^{-3} Ry/a.u.

III. RELAXED 6*H*-SiC(0001)-(1×1) SURFACES

Clean relaxed 6*H*-SiC(0001) surfaces, so far, have not been observed in experiment. At the unreconstructed Si-terminated (1×1) surface there is usually a disordered layer of impurities like O which can be removed by annealing in UHV. The C-terminated (1×1) surface results from impurities at the surface,[3] as well. For reference sake, we first address the clean relaxed 6*H*-SiC(0001)-(1×1) surfaces.

A top and a side view of the Si-terminated 6*H*-SiC(0001)-(1×1) substrate surface as resulting from our relaxation calculations is shown in Fig. 1. The parameters characterizing the relaxed structure are introduced in the figure, as well. Due to the hexagonal symmetry of the lattice only atomic relaxations along the surface vertical axis (z direction) can occur. For the relaxed C-terminated surface full dots and open circles have to be interchanged in Fig. 1. Table I shows the structure parameters for the optimally relaxed Si- and C-terminated substrate surfaces in comparison

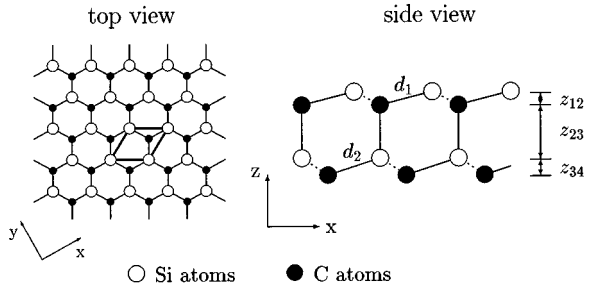

FIG. 1. Top and side view of the relaxed Si-terminated 6*H*-SiC(0001) surface. In this and in all following figures related to the surface structure, Si atoms are represented by open circles while C atoms are represented by black dots. Bonds lying in the drawing plane or parallel to it are shown by full lines and those forming an angle with the drawing plane are shown by dashed lines. The (1 ×1) unit cell is indicated by heavy lines and the labeling of characteristic structure parameters is introduced.

with the respective parameters of the ideal surfaces. The vertical distance between neighboring layers i and j is given by $z_{ij}= z_i - z_j$. The most significant effect to be observed is a pronounced inward relaxation of the top-layer atoms for both surfaces. The respective decrease of z_{12}, as compared to its value at the ideal surfaces, amounts to -0.15 Å for the Si- and -0.25 Å for the C-terminated surface. Concomitantly the bond lengths d_1 decrease by 0.04 Å and 0.07 Å, respectively, for the two surfaces. The relaxation-induced energy gain of 0.30 eV at the C-terminated surface is more than three times as large as that at the Si-terminated surface (0.09 eV) due to the larger relaxation of the C face. Bond-bending angular forces at the second-layer atoms are involved in these downward relaxations of the surface-layer atoms. They are considerably weaker at Si atoms than at C atoms so that the C-terminated surface shows the larger relaxation effects. The atomic relaxation on lower lying layers is very small.

Figure 2 shows the surface band structure for the relaxed Si- and C-terminated surfaces. The vertically shaded areas represent the (0001) projected bulk band structure (PBS) which is, of course, the same for both surfaces. The PBS has an indirect gap of 1.97 eV which is smaller than the experimental gap of 3.02 eV. This is due to the well-known underestimate of the band gap energy in LDA. For both Si- and C-terminated relaxed surfaces we find a dangling-bond band

TABLE I. Optimized structure parameters (as defined in Fig. 1) and energy difference per (1×1) unit cell between the ideal and the relaxed surface ΔE in comparison with the ideal surface parameters for the Si- and C-terminated 6*H*-SiC(0001) substrate surfaces.

	(1×1) ideal	Si-term. (1×1) relaxed	C-term. (1×1) relaxed
d_1 (Å)	1.88	1.84	1.81
d_2 (Å)	1.88	1.88	1.87
z_{12} (Å)	0.63	0.48	0.38
z_{23} (Å)	1.88	1.92	1.97
z_{34} (Å)	0.63	0.61	0.60
ΔE (eV)	0.00	−0.09	−0.30

in the gap energy region. These bands originate from the dangling bonds which are localized at the Si and C top-layer atoms, respectively. The dangling-bond band is half filled in both cases since there is only one top layer atom per (1 ×1) unit cell. The resulting band structures are thus metallic. Comparing the energetic positions of D_{Si} and D_{C} it becomes obvious that D_{C} occurs roughly 1.5 eV lower in energy than D_{Si}. This is due to the stronger C potential, as compared to the Si potential. This potential difference gives rise to the ionicity of SiC (see also Ref. 34), causing a charge transfer from the Si to the C atoms. The dispersion of D_{Si} is more pronounced than that of D_{C}, because D_{Si} is laterally more extended. This can be seen in Fig. 3, which shows the charge densities of the dangling-bond states D_{Si} and D_{C}. They clearly reveal that the dangling bonds are predominantly localized at the top-layer atoms and are oriented perpendicularly to the surface. The charge densities of the two dangling-bond states, however, show significant differences. While D_{Si} is predominantly directed outward into vacuum, the maximum of D_{C} is directed towards the substrate. This could originate from the stronger relaxation of the C-terminated surface.

IV. RECONSTRUCTED 6*H*-SiC(0001) -($\sqrt{3}\times\sqrt{3}$) SURFACES

A. Adsorption-induced reconstructions of the Si-terminated substrate

The $\sqrt{3}\times\sqrt{3}$ unit cell is three times as large as that of the relaxed surfaces and contains three atoms per layer unit cell

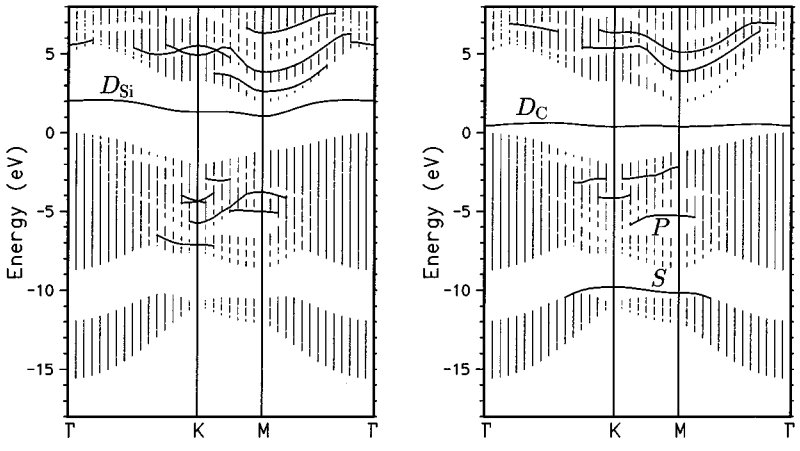

FIG. 2. Surface band structures of the relaxed Si-terminated (left panel) and C-terminated (right panel) 6*H*-SiC(0001)-(1×1) surfaces. The projected bulk band structure is shown by vertically shaded areas.

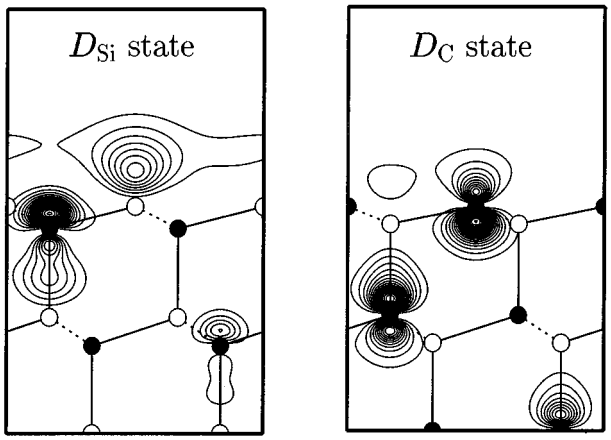

FIG. 3. Charge density contours of the dangling-bond states at the Γ point for the relaxed Si-terminated (left panel) and C-terminated (right panel) 6H-SiC(0001)-(1×1) surfaces. The charge densities are presented for a side view of the relaxed structures (see also Fig. 1).

in the substrate. The STM measurements of Owman and Mårtensson[9] for the Si-terminated 6*H*-SiC(0001)-($\sqrt{3}\times\sqrt{3}$)*R*30° surface have yielded images similar to the Si(111) surface covered with 1/3 monolayer of Al, Ga, In, or Pb. Stimulated by this work we have investigated five adsorption models of the Si-terminated 6*H*-SiC(0001)-($\sqrt{3}\times\sqrt{3}$)*R*30° surface. They are shown in Fig. 4 by top and side views. The structure parameters characterizing the different configurations are introduced in Fig. 4, as well. We have considered Si adatoms in T_4 [Fig. 4(a)] and H_3 [Fig. 4(b)] and C adatoms in T_4 positions [Fig. 4(c)]. In addition, we have optimized Si and C trimers in T_4 positions [Figs. 4(d) and 4(e)]. Adatoms in T_4 (H_3) positions reside above second (fourth) substrate-layer atoms [see, e.g., Figs. 4(a) and 4(b)]. For the sake of brevity, we will refer to the different configurations as Si(T_4), Si(H_3), etc. The resulting optimal structures obtained from our total-energy minimization are drawn to scale in Figs. 4(a)–4(e).

1. Surface structure

In all five adsorption configurations the three substrate-surface dangling bonds per $\sqrt{3}\times\sqrt{3}$ unit cell become fully saturated by the adatoms. But now the adatoms have dangling bonds. Their number, however, is smaller than the number of the original dangling bonds at the clean substrate surface. In the configurations of Figs. 4(a)–4(c) the number of dangling bonds is reduced by adatom adsorption to one third. In the case of the Si and C trimers [see Figs. 4(d) and 4(e)] the dangling-bond reduction sensitively depends on to which extent the dangling bonds at the trimer atoms become involved in chemical bonding.

The newly established surface bonds d_1 have a bond length which turns out to be slightly larger than respective bulk bonds (2.33 Å for Si and 1.88 Å for SiC) and close to the sum of the covalent radii of the involved atoms (r_C=0.77 Å and r_{Si}=1.17 Å). The new surface bonds are significantly strained, however, since the respective bond angle α (see Fig. 4 and Table II) is far from the tetrahedral

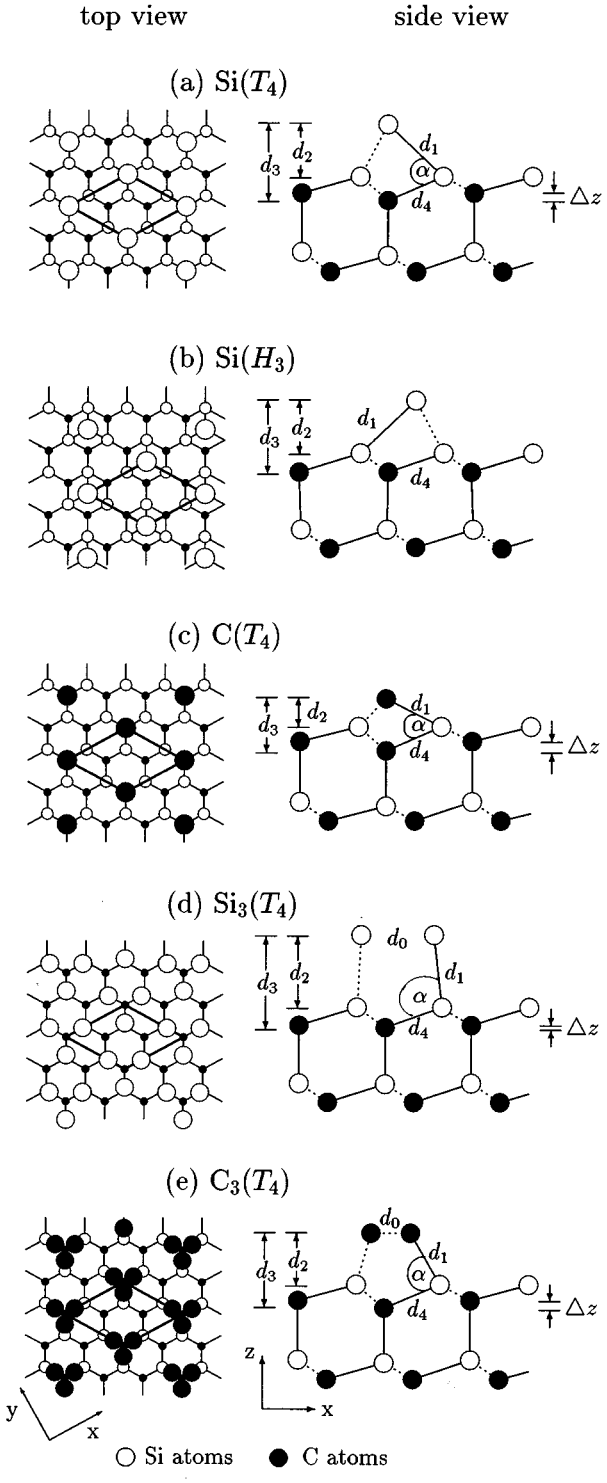

FIG. 4. Top and side views of the optimized ($\sqrt{3}\times\sqrt{3}$)*R*30° reconstructions of Si-terminated 6*H*-SiC(0001) surfaces. The $\sqrt{3}\times\sqrt{3}$ unit cells are indicated by heavy lines in the left panels. The structure parameters are introduced in the side views (see also caption of Fig. 1).

angle of 109.5°. There is an important difference between the T_4 and H_3 configurations to be noted at this point. In the T_4 configuration, the system can reduce its strain and increase the bond angle α by pushing down the second-layer C atom residing vertically below the adatom and lifting the other two C atoms in the $\sqrt{3}\times\sqrt{3}$ unit cell on the second

TABLE II. Optimized structure parameters (as defined in Fig. 4) for the Si and C adatom and Si and C trimer reconstructions of the Si-terminated $6H$-SiC(0001)-($\sqrt{3}\times\sqrt{3}$)$R30°$ surfaces adressed in this work. The values in parentheses are the results of Ref. 25.

	Adsorption models for the Si-terminated $\sqrt{3}\times\sqrt{3}$ surface				
	Si(T_4)	Si(H_3)	C(T_4)	Si trimer(T_4)	C trimer(T_4)
d_0 (Å)				2.59	1.41
d_1 (Å)	2.41 (2.42)	2.44	1.93 (1.98)	2.39	1.92
d_2 (Å)	1.71 (1.75)	1.73	0.92 (1.22)	2.37	1.69
d_3 (Å)	2.50	2.36	1.70	3.03	2.46
d_4 (Å)	1.88	1.88	1.87	1.87	1.89
Δz (Å)	0.25 (0.22)		0.31 (0.52)	0.07	0.25
α(°)	70		53	105	86

substrate layer. In consequence, a buckling of the second substrate layer, characterized by Δz (see Fig. 4 and Table II) occurs. In the H_3 configuration, on the contrary, all three C atoms per unit cell on the second substrate layer are equivalent so that no buckling of the second layer can occur. Thus strain relief can be accomplished much more efficiently in the T_4 than in the H_3 configuration.

In our optimized Si(T_4) structure each Si adatom forms a bond of length $d_1=2.41$ Å [see Fig. 4(a) and Table II] with each of the three Si substrate-surface layer atoms. This bond length is larger than the Si-Si bulk-bond length of 2.33 Å. The three Si surface atoms in the $\sqrt{3}\times\sqrt{3}$ unit cell slightly shift in the direction of the adatoms. By pushing down the second-layer C atom residing below the adatom and lifting the other two C atoms on the second substrate layer the bond angle α increases to 70°. So a buckling of $\Delta z=0.25$ Å occurs. The relaxation of the atoms on the third and fourth layer is smaller than 0.09 Å. The bond lengths d_4 between the first and second substrate-layer atoms result as bulklike.

The numbers in parentheses in Table II are the LDA results of Northrup and Neugebauer.[25] The agreement between their results and ours for Si adatoms in T_4 positions is very close.

Figure 4(b) shows our optimized Si(H_3) structure by a top and a side view. The respective structure parameters are given in Table II, as well. The bond lengths d_1, d_2, and d_4 for Si(H_3) are very similar to those for the optimized Si(T_4) configuration. The discerning feature of the two configurations is the buckling $\Delta z=0.25$ Å in the second substrate layer which can occur only for adatoms in T_4 positions. The Si(H_3) configuration turns out to be energetically less favorable than the Si(T_4) configuration by $\Delta E=0.60$ eV per $\sqrt{3}\times\sqrt{3}$ unit cell. This result is in very close agreement with the respective energy difference of $\Delta E=0.54$ eV, reported in Ref. 25.

When C adatoms are adsorbed in T_4 positions, the bond length of $d_1=1.93$ Å between the C adatoms and the Si substrate surface-layer atoms is smaller than that for the Si adatoms because of the smaller covalent radius of carbon. The distance of the C adatoms to the second-layer C atoms turns out to be only $d_3=1.70$ Å. In consequence, the second substrate-layer buckling Δz is as large as 0.31 Å in our results. The surface bonds are very strongly strained since d_3 is very small and α turns out to be only 53°. Because of their smaller covalent radius the C adatoms in C(T_4) reside nearer to the Si substrate-surface atoms than the Si adatoms in Si(T_4). Northrup and Neugebauer[25] have found a similar bond length between the C adatoms and the Si surface-layer atoms. But in their optimized configuration the C atoms in the second substrate layer residing vertically below the C adatoms show a larger relaxation towards the substrate. The authors find a buckling of $\Delta z=0.52$ Å which is larger than our respective value. These differences may be related to slight differences in technical details (basis sets, number of special points used in the Brillouin-zone integrations, pseudopotentials, and slab geometries) which can be expected to be more pronounced for C adatoms than for Si adatoms since the C potential is more strongly structured than the Si potential and the C orbitals are more localized than the Si orbitals.

When Si trimers are adsorbed in T_4 positions at the substrate surface, we observe that the individual Si atoms of the trimers move into new positions vertically above the Si substrate surface atoms [see Fig. 4(d)]. In the optimized configuration their lateral distance of 2.59 Å is considerably larger than twice the covalent radius of Si or the Si-Si bulk-bond length of 2.33 Å, respectively. Therefore in Fig. 4(d) no bond was drawn between the Si adlayer atoms in the optimized configuration. The structure parameters are shown in Table II. The bonding configuration is nearly tetrahedal, resulting in an angle of $\alpha=105°$ and a concomitantly small buckling $\Delta z=0.07$ Å of the second substrate layer. The bond length d_1 between the Si adatoms and the Si substrate-surface-layer atoms of 2.39 Å is close to the bulk-bond length of Si and to the sum of the covalent radii of two Si atoms.

When C trimers are adsorbed in T_4 positions the resulting C-Si bond length $d_1=1.92$ Å is again close to the sum of the covalent radii of C and Si. The three C trimer atoms saturate the substrate-surface dangling bonds and form C-C bonds with a bond length of $d_0=1.41$ Å. This value is between the length of C=C double bonds (1.36 Å) in molecules and C-C single bonds (1.52 Å) in bulk diamond. The bond angle $\alpha=86°$ is closer to the tetrahedal angle than for the Si(T_4) and C(H_3) adatom geometries. Because of the smaller strain in the bonds, the buckling of the C atoms in the second substrate layer ($\Delta z=0.25$ Å) is smaller than for the C(T_4) structure ($\Delta z=0.31$ Å).

If we adsorb, instead, a full C monolayer in on top positions above Si substrate-surface-layer atoms the C atoms

become onefold coordinated to the substrate and exhibit three dangling bonds each. This configuration is very unfavorable (by 11 eV per unit cell), as compared to our optimized $C_3(T_4)$ configuration. Badziag favored this type of configuration[24] containing, however, H atoms saturating the C adatom dangling bonds.

2. Determination of optimal surface structure for the Si-terminated substrate surface

The different optimized adsorption models cannot directly be compared in a meaningful way since the number (one or three) and the species (Si or C) of the adatoms are different. Nevertheless, we can compare the energies of the different structures using the grand canonical potential at $T=0$ K, as suggested by Qian, Martin, and Chadi[37] and by Northrup and Froyen:[38]

$$\Omega = E - \sum_i \mu_i n_i .$$

The μ_i are the chemical potentials of atomic species i and n_i is the number of atoms i in the system. Now, if a system consisting of a SiC crystal and Si and C atoms in the gas phase is in thermodynamic equilibrium, the following relation holds:

$$\mu_{\mathrm{Si}} + \mu_{\mathrm{C}} = \mu_{\mathrm{SiC(bulk)}} .$$

In addition, the following relation holds:

$$\mu_{\mathrm{SiC(bulk)}} = \mu_{\mathrm{Si(bulk)}} + \mu_{\mathrm{C(bulk)}} - \Delta H_f .$$

Here μ_{Si} and μ_{C} are the chemical potentials of the free atoms in the gas phase while $\mu_{\mathrm{Si(bulk)}}$, $\mu_{\mathrm{C(bulk)}}$, and $\mu_{\mathrm{SiC(bulk)}}$ are the chemical potentials of the atoms in the respective bulk crystals. Finally, ΔH_f is the formation enthalpy of the SiC bulk crystal. The above relation allows one to eliminate μ_{C} in the grand canonical potential. Thus we can evalute Ω as a function of the chemical potential of the involved Si atoms, alone. The formation enthalpy ΔH_f results as $\Delta H_f = 0.51$ eV in our calculations. Northrup and Neugebauer[25] obtained a value of 0.75 eV in their calculations. The experimental value is 0.72 eV.

The chemical potential μ_{Si} is restricted to the range[37,38]

$$\mu_{\mathrm{Si(bulk)}} - \Delta H_f \leqslant \mu_{\mathrm{Si}} \leqslant \mu_{\mathrm{Si(bulk)}} .$$

In Fig. 5 we show the change in Ω relative to its value for the ideal surface for the six different configurations studied as a function of μ_{Si}. Obviously, C adatoms and C trimers are less favorable than the ideal Si-terminated surface. This result derives from the fact that C adatoms are too small to efficiently saturate the dangling bonds on the Si substrate-surface-layer atoms, as has been pointed out already by Northrup and Neugebauer.[25] In particular, the bonds between C adatoms and Si substrate-surface-layer atoms are far from tetrahedral and thus strongly strained. The relaxation of the ideal surface slightly lowers the energy. $\mathrm{Si}(H_3)$ and $\mathrm{Si}(T_4)$ configurations are more favorable. The energetic order of $\mathrm{Si}(T_4)$ and $\mathrm{C}(T_4)$ corresponds to the size of the bond angle α which is 70° and 53°, respectively, in the two cases (see Table II). Note that the change in Ω increases (decreases) for adsorbed C (Si) atoms as a function of μ_{Si}.

From our analysis we conclude that the Si-terminated $6H$-SiC(0001) surface shows a $\sqrt{3}\times\sqrt{3}$ reconstruction if Si and C atoms are offered in the gas phase. Our conclusion and our actual $\mathrm{Si}(T_4)$ structure are compatible with experimental data[3,4,6,7,9,11] and in very good agreement with the LDA results of Northrup and Neugebauer.[25]

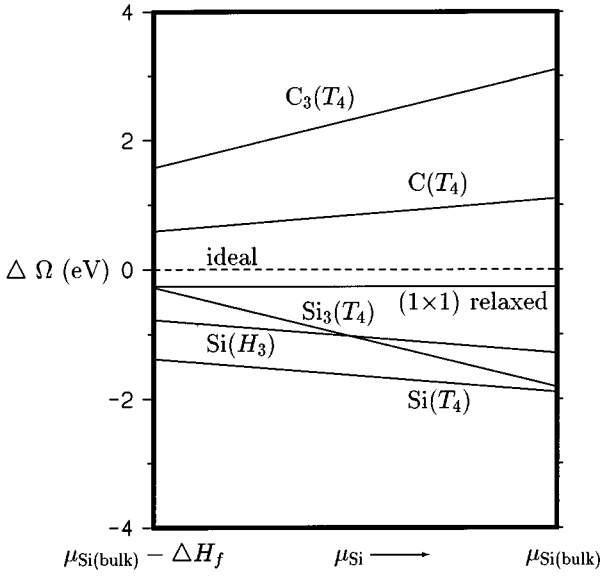

FIG. 5. Comparison of grand canonical potentials (relative to that of the ideal surface) for six different structural models (relaxation and five different reconstructions) of the Si-terminated $6H$-SiC(0001)-$(\sqrt{3}\times\sqrt{3})R30°$ surface as a function of the Si chemical potential μ_{Si} for the allowed range.

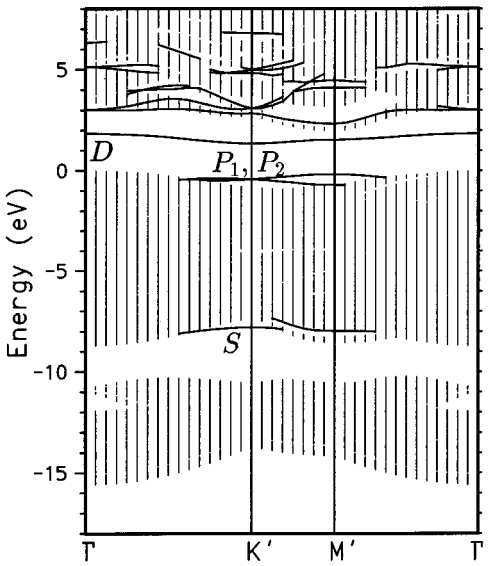

FIG. 6. Surface band structure of the Si-terminated $6H$-SiC(0001)-$(\sqrt{3}\times\sqrt{3})R30°$ surface for Si adatoms in T_4 position [see Fig. 4(a)]. The projected bulk band structure for the $\sqrt{3}\times\sqrt{3}$ SBZ is shown by vertically shaded areas.

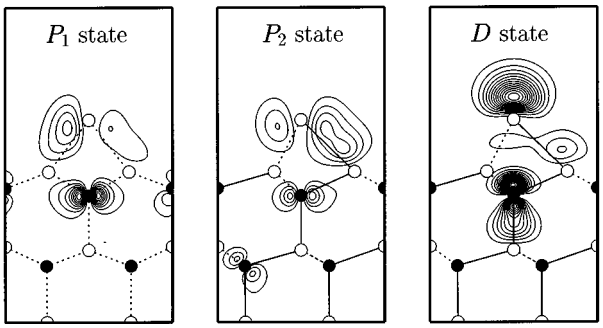

FIG. 7. Charge density contours of salient surface states at the M' point of the $(\sqrt{3}\times\sqrt{3})R30°$ SBZ of the Si-terminated $6H$-SiC(0001)-$(\sqrt{3}\times\sqrt{3})R30°$ surface for Si adatoms in T_4 position. The charge density of the P_1 state is presented in the y-z plane (see Fig. 4). The charge densities of the P_2 and D states are presented in the x-z plane containing the middle Si-C zigzag chain (see also caption of Fig. 1).

3. Surface electronic structure

We have calculated the surface electronic structure for all optimized adsorption models of the Si-terminated $6H$-SiC(0001)-$(\sqrt{3}\times\sqrt{3})R30°$ surface. For the sake of brevity, we restrict ourselves to a discussion of the surface band structure and salient charge densities for the energetically optimal Si(T_4) configuration [see Figs. 4(a) and 5–7]. Concerning the surface band structures of the other models studied, the interested reader is referred to Ref. 39. Figure 6 shows the PBS of the $(\sqrt{3}\times\sqrt{3})R30°$ SBZ by vertically dashed lines. Bands of localized surface states and of surface resonances are shown by full lines. Within the projected gap energy region we find three bands of localized states. The bands P_1 and P_2 with p_x and p_y symmetry originate from the interaction of the Si(T_4) adatoms with the Si substrate-surface-layer atoms (see Fig. 7). The band D having mostly p_z wave-function character originates from the dangling-bond states localized at the Si(T_4) adatoms (see Fig. 7). The dispersion of the D band is very small because the Si adatoms have a large distance of 5.32 Å and thus interact only very weakly. The dangling-bond charge density shows a strong contribution at the C atoms that reside on the second substrate layer vertically below the Si adatoms in T_4 positions. The dangling-bond-derived band D is half filled since there is only one adatom per $\sqrt{3}\times\sqrt{3}$ unit cell. The resulting band structure is metallic, therefore. The metallic nature of this surface, as resulting from our calculations, is in agreement with the theoretical results of Ref. 25. Contrary to these theoretical results, recent ARPES (Ref. 17) and KRIPES (Ref. 18) investigations have observed a band of occupied and a band of empty dangling-bond states in the gap energy region, respectively. In both Refs. 17 and 18 the authors conclude on the basis of their data that the surface is semiconducting. This is an obvious contradiction between theory and experiment which calls for further investigations. One possible reason for the discrepancy could be the fact that the actual structure of this surface is more complex than we have anticipated so far. Adatoms with five valence electrons, e.g., instead of Si adatoms would lead to a semiconducting surface. In such a case a fully occupied dangling-bond band would result within the gap. But no empty dangling-bond band would occur, in contrast to the observation of Themlin *et al.*[18] Another possible explanation could be related to many-body correlation effects of the Hubbard type in the dangling-bond band giving rise to a splitting of the D band. This would result in an occupied and an empty dangling-bond band within the gap energy region. These topics have been briefly addressed already in Refs. 17, 18, and 25. Certainly, more work is needed in this field to resolve the issue.

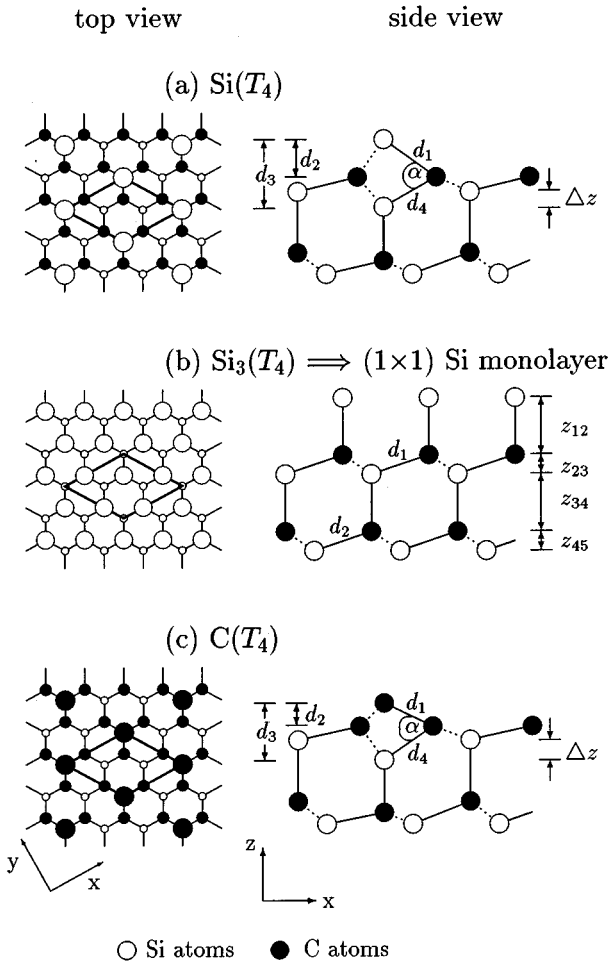

FIG. 8. Top and side views of the optimized $(\sqrt{3}\times\sqrt{3})R30°$ reconstructions of the C-terminated $6H$-SiC(0001) surfaces. The structure parameters are introduced in the side views (see also caption of Fig. 4).

B. Adsorption-induced reconstructions of the C-terminated substrate

We have also investigated several $(\sqrt{3}\times\sqrt{3})R30°$ reconstruction models of the C-terminated substrate surface. Three different adsorption configurations have been optimized. We have considered Si and C adatoms in T_4 position [Figs. 8(a) and 8(c)] and Si trimers in T_4 position [Fig. 8(b)]. The resulting optimal structures obtained from our total-energy minimization are shown in Figs. 8(a)–8(c) by top and side views. The relevant structure parameters are defined in the figure. In experiment there seemed to be no indication of a $(\sqrt{3}\times\sqrt{3})R30°$ reconstruction for the C-terminated

TABLE III. Optimized structure parameters (as defined in Fig. 8) for the C and Si adatom and Si trimer reconstructions of the C-terminated 6*H*-SiC(0001)-($\sqrt{3}\times\sqrt{3}$)*R*30° surfaces addressed in this work. Adsorption of Si trimers leads to an ideal (1×1) structure in our calculations, in which the Si surface atoms are onefold coordinated with the C substrate-surface-layer atoms and have three unsaturated dangling bonds each.

	Adsorption models for the C-terminated $\sqrt{3}\times\sqrt{3}$ surface		
	C(T_4)	Si(T_4)	Si trimer(T_4)
d_0 (Å)			3.07
d_1 (Å)	1.66	2.04	1.88
d_2 (Å)	0.73	1.24	1.88
d_3 (Å)	1.86	2.21	2.51
d_4 (Å)	1.87	1.89	1.88
Δz (Å)	0.68	0.50	0.00
α(°)	63	68	109.5

surface[3,6] until very recently when the STM results of Li and Tsong[11] were published. For this termination rather (3×3) reconstructions or impurity-stabilized (1×1) structures were mostly observed.

1. Surface structure

First we discuss our results for the adsorption of Si and C adatoms in T_4 position on the C-terminated 6*H*-SiC(0001) surface. The optimized structure is shown in Figs. 8(a) and 8(c) by top and side views. The structure parameters are given in Table III. At this surface, the C(Si) adatoms are bound to three substrate-surface-layer atoms. The respective C-C and Si-C bond lengths d_1 (see Table III) are somewhat larger than respective bulk-bond lengths of diamond (1.52 Å) and of SiC (1.88 Å). In both Si(T_4) and C(T_4) configurations the resulting distances d_2 between adatoms and Si atoms in the second substrate layer are relatively small because of the very small covalent radius of C. In consequence, a large buckling Δz of the second substrate layer results. The Si atoms on this second substrate layer show a much larger buckling than the C atoms on the corresponding second layer of the Si-terminated surface (see Table II). These differences are again related to the differences in angular forces at the C or Si atoms which are involved in the reconstruction-induced bond bending.[40] Correspondingly, the bond angle α is 68° for Si(T_4) at the C-terminated surface while it is only 53° for C(T_4) at the Si-terminated surface. The bonds are less strained in the former case, therefore.

For Si trimers adsorbed in T_4 positions we obtain an unexpected result. It turns out that upon energy minimization the Si atoms move to ideal on top positions above the C atoms at the substrate-surface layer and a geometrically ideal (1×1) structure results. But in this structure the Si adatoms are only onefold coordinated to the substrate and thus have three unsaturated dangling bonds, each. Finally we note that in all reconstructions considered in our work the bond lengths d_4 between Si and C atoms on the first and second substrate layers are nearly the same as in bulk 6*H*-SiC.

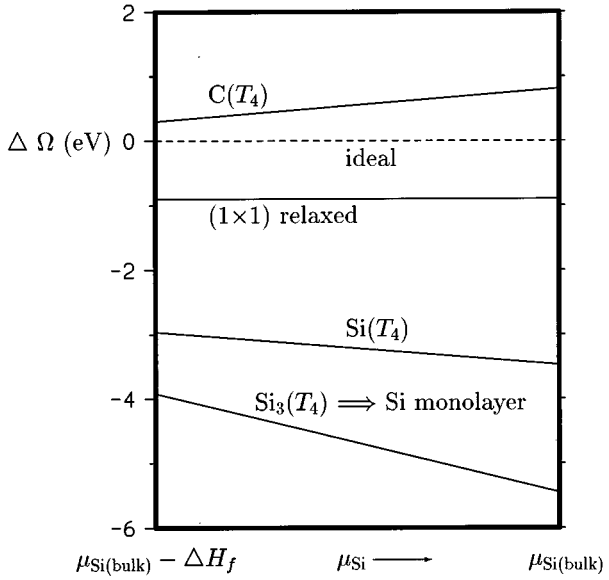

FIG. 9. Comparison of grand canonical potentials (relative to that of the ideal surface) for four different structural models (relaxation and three different reconstructions) of the C-terminated 6*H*-SiC(0001)-($\sqrt{3}\times\sqrt{3}$)*R*30° surface as a function of the chemical potential μ_{Si} for the allowed range (for details, see text).

2. Determination of optimal surface structure for the C-terminated surface

In Fig. 9 we show the change in the grand canonical potential Ω relative to its value for the ideal surface for the investigated structures as a function of μ_{Si}. Similar to the case of the Si-terminated substrate surface, C adatoms turn out to be less favorable than the ideal surface structure. The relaxation of the ideal surface reduces the total energy in this case more than for the Si-terminated surface. The Si(T_4) configuration is, however, considerably more stable for all values of μ_{Si}. The grand canonical potential is even lower than that for the Si(T_4) configuration (see Fig. 5) of the Si-terminated substrate surface.

Concerning the Si monolayer which results from adsorbed Si trimers after energy minimization it turns out that it is energetically most favorable. In this case there are three equivalent adatoms per $\sqrt{3}\times\sqrt{3}$ unit cell while in the Si(T_4) configuration there is only one adatom per unit cell. The Si monolayer gives rise to a (1×1) structure in which the Si adlayer atoms have three unsaturated dangling bonds each. Considering the grand canonical potential we have to compare the energies of three Si adatoms adsorbed in ideal onefold-coordinated sites, having three dangling bonds each, with one Si adatom adsorbed in a T_4 site of the $\sqrt{3}\times\sqrt{3}$ unit cell and two free Si atoms in the gas phase. Although the Si(T_4) adatom is stronger bound than each Si adatom in the ideal (1×1) configuration, the monolayer system has the lower grand canonical potential.

Our results clearly show that the investigated $\sqrt{3}\times\sqrt{3}$ structures of the C-terminated surface are no minimum configurations. Instead, an adsorbed Si monolayer turns out to be energetically much more favorable. It seems obvious, however, that such a monolayer is not stable since each adlayer

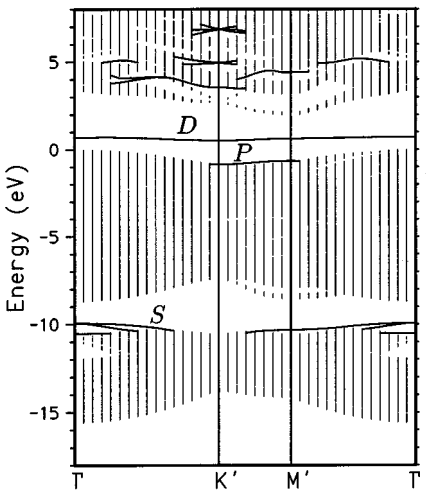

FIG. 10. Surface band structure of the C-terminated $6H$-SiC(0001)-$(\sqrt{3}\times\sqrt{3})R30°$ surface for Si adatoms in T_4 position [see Fig. 8(a)].

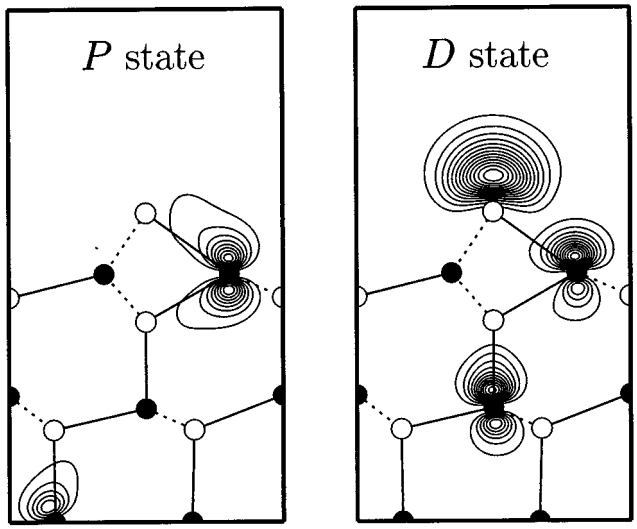

FIG. 11. Charge density contours of salient surface states at the M' point of the SBZ of the C-terminated $6H$-SiC(0001)-$(\sqrt{3}\times\sqrt{3})R30°$ surface for Si adatoms in T_4 position. The charge densities are presented in the x-z plane containing the middle Si-C zigzag chain (see Fig. 8).

Si atom has three unsaturated dangling bonds in this (1×1) configuration. A more complicated reconstruction is therefore to be expected. This conclusion is in accord with experiment, which has observed (3×3) reconstructions[6–8] of this surface. To study more extended (3×3) reconstructions one would have to consider slabs with nine atoms per layer unit cell. We have, so far, not yet addressed such large reconstructions. Another possibility could be a $\sqrt{3}\times\sqrt{3}$ B_5 model, as discussed in Refs. 11 and 23, in which Si adatoms are adsorbed in T_4 positions above the C-terminated surface and all second-layer substrate Si atoms are replaced by C atoms. Also impurity-stabilized (1×1) structures, as observed by Bermudez,[3] should be considered in this context.

3. Surface electronic structure

In the discussion of the electronic structure of the C-terminated $6H$-SiC(0001)$(\sqrt{3}\times\sqrt{3})R30°$ surfaces we concentrate on the optimized Si(T_4) adatom configuration. The surface band structure for this configuration is shown in Fig. 10. The electronic surface structure for the other optimized adsorption geometries of C-terminated $6H$-SiC(0001) surfaces is given in Ref. 39.

We address this surface band structure for the sake of comparison with Fig. 6 although the Si(T_4) configuration of the C-terminated surface obviously is not the energy minimum configuration. In the gap energy region we find an occupied valence band P and a half-occupied dangling-bond band D. Comparing these bands with those in Fig. 6 it becomes obvious that they result roughly 1 eV lower in energy than the corresponding bands at the Si-terminated surface. This originates from the stronger C potentials on the substrate-surface layer of the C-terminated substrate as compared to the Si potentials on the substrate-surface layer of the Si-terminated substrate. The related charge density (see Fig. 11) of the dangling-bond state D is localized at the Si(T_4) adatoms but shows a strong coupling to the C atoms on the first and third substrate layers, in addition. This is significantly different from the respective coupling of the D state in Fig. 7.

V. SUMMARY

We have reported *ab initio* studies of relaxed and $\sqrt{3}\times\sqrt{3}$ reconstructed $6H$-SiC(0001) surfaces. For the relaxed surfaces, we find an inward relaxation of the top-layer atoms towards the substrate in both cases. This top-layer relaxation is larger at the C-terminated (-0.25 Å) than at the Si-terminated (-0.15 Å) (1×1) surface. For the $\sqrt{3}\times\sqrt{3}$ reconstruction at the Si-terminated substrate surface, our results favor Si adatoms in T_4 positions with a distance of 2.44 Å to the Si atoms in the top layer of the substrate. This is in close agreement with the results of a complementary *ab initio* calculation.[25] The optimal Si(T_4) geometry is also more favorable than the relaxed Si-terminated (1×1) surface configuration. Our optimal Si(T_4) structure is compatible with experiment, which finds an ordered arrangement of Si vacancies in a chemisorbed Si layer on the $(\sqrt{3}\times\sqrt{3})R30°$ reconstruction.[3] The $\sqrt{3}\times\sqrt{3}$ reconstructions of the C-terminated substrate surface which we have studied turn out to be energetically less favorable than a full monolayer of Si adsorbed in a (1×1) configuration. In the latter structure, the Si adatoms are onefold coordinated to the substrate and they have three unsaturated dangling bonds, each. This structure, certainly, is not expected to be stable. A more complex reconstruction such as, e.g., a (3×3) structure or possibly a $\sqrt{3}\times\sqrt{3}$ B_5 structure is to be expected. This would be compatible with recent experimental data for the C-terminated substrate surface.[3,6,11]

All configurations for the relaxed and the $(\sqrt{3}\times\sqrt{3})R30°$ reconstructed surfaces which we have investigated have a metallic nature. This is caused by the fact that there is an odd number of valence electrons per surface-layer

unit cell, in each case, which can only partially occupy the dandling-bond bands in the gap energy region. For the case of the Si-terminated substrate this finding is in contradiction to experiment, which observes the $(\sqrt{3}\times\sqrt{3})$ surface to be semiconducting.[17,18] These conflicting results mean that either the optimal structure for this surface is more complicated than anticipated in our work or that many-body correlation effects give rise to a splitting of the dangling-bond bands. Another possibility to arrive at semiconducting surfaces would be adatoms other than Si or C with an odd number of valence electrons. These open questions call for further studies of more extended reconstructions or of impurity-stabilized surfaces which are beyond the scope of our current calculations.

ACKNOWLEDGMENT

One of us (M.S.) would like to acknowledge support by the Bischöfliche Studienförderung Cusanuswerk (Bonn, Germany).

[1] G. L. Harris, in *Properties of Silicon Carbide*, edited by G. L. Harris, EMIS Datareviews Series No. 13 (INSPEC, London, 1995).
[2] P. A. Ivanov and V. E. Chelnokov, Semicond. Sci. Technol. **7**, 863 (1992).
[3] V. M. Bermudez, Appl. Surf. Sci. **84**, 45 (1995).
[4] R. Kaplan, Surf. Sci. **215**, 111 (1989).
[5] A. J. van Bommel, J. E. Crombeen, and A. van Tooren, Surf. Sci. **48**, 463 (1975).
[6] S. Nakanishi, H. Tokutaka, K. Nishimori, S. Kishida, and N. Ishihara, Appl. Surf. Sci. **41/42**, 44 (1989).
[7] U. Starke, Ch. Bram, P.-R. Steiner, W. Hartner, L. Hammer, K. Heinz, and K. Müller, Appl. Surf. Sci. **89**, 175 (1995).
[8] J. Schardt, Ch. Bram, S. Müller, U. Starke, K. Heinz, and K. Müller, Surf. Sci. **337**, 232 (1995).
[9] F. Owman and P. Mårtensson, Surf. Sci. **330**, L639 (1995).
[10] L. Muehlhoff, W. J. Choyke, M. J. Bozack, and J. T. Yates, Jr., J. Appl. Phys. **60**, 2842 (1986).
[11] L. Li and I. S. T. Tsong, Surf. Sci. **351**, 141 (1996).
[12] C. S. Chang, I. S. T. Tsong, Y. C. Wang, and R. F. Davis, Surf. Sci. **256**, 354 (1991).
[13] M. A. Kulakov, P. Heuell, V. F. Tsvetkov, and B. Bullemer, Surf. Sci. **315**, 248 (1994).
[14] M. A. Kulakov, G. Henn, and B. Bullemer, Surf. Sci. **346**, 49 (1996).
[15] S. Tyc, J. Phys. (France) I **4**, 617 (1994).
[16] L. I. Johansson, F. Owman, and P. Mårtensson, Phys. Rev. B **53**, 13 793 (1996).
[17] L. I. Johansson, F. Owman, P. Mårtensson, C. Persson, and U. Lindefelt, Phys. Rev. B **53**, 13 803 (1996).
[18] J.-M. Themlin, I. Forbeaux, V. Langlais, H. Belkhir, and J.-M. Debever (unpublished).
[19] R. J. Hamers, Phys. Rev. B **40**, 1657 (1989).
[20] J. Nogami, S.-I. Park, and C. F. Quate, Phys. Rev. B **36**, 6221 (1987).
[21] J. Nogami, S.-I. Park, and C. F. Quate, Surf. Sci. **203**, L631 (1988).
[22] E. Ganz, I.-S. Hwang, F. Xiong, S. K. Theiss, and J. Golovchenko, Surf. Sci. **257**, 259 (1991).
[23] P. Badziag, Surf. Sci. **236**, 48 (1990).
[24] P. Badziag, Surf. Sci. **337**, 1 (1995).
[25] J. E. Northrup and J. Neugebauer, Phys. Rev. B **52**, R17 001 (1995).
[26] M. Sabisch, P. Krüger, A. Mazur, and J. Pollmann, Surf. Rev. Lett. (to be published).
[27] M. Sabisch, P. Krüger, A. Mazur, and J. Pollmann, in *Proceedings of ICPS-23*, edited by M. Scheffler and R. Zimmermann (World Scientific, Singapore, 1996), p. 819.
[28] P. Hohenberg and W. Kohn, Phys. Rev. B **136**, B864 (1964); W. Kohn and L. J. Sham, *ibid.* **140**, A1133 (1965).
[29] D. M. Ceperley and B. I. Alder, Phys. Rev. Lett. **45**, 566 (1980).
[30] J. P. Perdew and A. Zunger, Phys. Rev. B **23**, 5048 (1981).
[31] L. Kleinman and D. M. Bylander, Phys. Rev. Lett. **48**, 1425 (1982).
[32] D. R. Hamann, M. Schlüter, and C. Chiang, Phys. Rev. Lett. **43**, 1494 (1979).
[33] M. Sabisch, Diploma thesis, Universität Münster, 1993.
[34] M. Sabisch, P. Krüger, and J. Pollmann, Phys. Rev. B **51**, 13 367 (1995).
[35] M. Sabisch, P. Krüger, A. Mazur, M. Rohlfing, and J. Pollmann, Phys. Rev. B **53**, 13 121 (1996).
[36] J. Ihm, A. Zunger, and M. L. Cohen, J. Phys. C **12**, 4409 (1979).
[37] G.-X. Qian, R. M. Martin, and D. J. Chadi, Phys. Rev. B **38**, 7649 (1988).
[38] J. E. Northrup and S. Froyen, Phys. Rev. Lett. **71**, 2276 (1993).
[39] M. Sabisch, Ph.D. thesis, Universität Münster, 1996.
[40] J. Pollmann, P. Krüger, M. Rohlfing, M. Sabisch, and D. Vogel, Proceedings of ICFSI-5, edited by A. Kahn and R. Lüdeke [Appl. Surf. Sci. **104/105**, 1 (1996)].